

# Optical properties of perovskite alkaline earth titanates : a formulation

**Kamal Krishna Saha, Tanusri Saha-Dasgupta and Abhijit Mookerjee**

S. N. Bose National Centre for Basic Sciences. Block-JD, Sector-III, Kolkata-700098, India.

**Sonali Saha and T.P. Sinha**

Department of Physics, J.C. Bose Institute, 93/1 Acharya Prafulla Chandra Road, Kolkata-700009, India

**Abstract.** In this communication we suggest a formulation of the optical conductivity as a convolution of an energy resolved joint density of states and an energy-frequency labelled transition rate. Our final aim is to develop a scheme based on the augmented space recursion for random systems. In order to gain confidence in our formulation, we apply the formulation to three alkaline earth titanates  $CaTiO_3$ ,  $SrTiO_3$  and  $BaTiO_3$  and compare our results with available data on optical properties of these systems.

E-mail: [kamal@bose.res.in](mailto:kamal@bose.res.in)

PACS numbers: 71.20,71,20c

## 1. Introduction

The object of our present study is to derive an expression for the optical conductivity as a convolution of the energy resolved joint density of states and an energy-frequency dependent transition rate. The need is to go beyond the usual reciprocal space based formulations and obtain an expression which we can immediately generalize for disordered systems. This would require labelling states by energy and the angular momentum labels  $(\ell, m)$  alone. Once we derive this expression we shall find a representation for the optical conductivity in the minimal basis set of the tight-binding linearized muffin-tin orbitals (TB-LMTO). The generalization to disordered systems will be carried out through the augmented space recursion (ASR) introduced by us earlier for the study of electronic properties of disordered systems [1]-[5]. The ASR carries out the configuration averaging essential to the description of properties of disordered systems, going beyond the usual mean-field approaches and taking into account configuration fluctuations. The input into the ASR method includes the Hamiltonian parameters of the pure constituents, as the starting point of the local spin density approximation (LSDA) iterations for the alloy. It also includes the information about the transition rates of the pure constituents, expressed as functions of the initial and final state energies. The aim of this paper is to reformulate the reciprocal space representation of the transition rate and re-express it in the energy-frequency label representation for the pure constituents. Only when we are confident that this works, can we proceed with the full calculations for the disordered alloy. This communication is an attempt to verify our formulation for a series of alkaline earth titanates in the paraelectric phase, on which extensive theoretical and experimental data of optical properties are available for comparison.

Perovskite structured titanate ferroelectric compounds is, to date, one of the most extensively investigated materials. They are extremely interesting from the viewpoint of solid state theoreticians because their structures are a lot simpler than that of any other ferroelectric material known, and, therefore, prove to be rather simple systems to study and better understand the ferroelectric phenomenon. The titanates are very easily prepared as polycrystalline ceramics, they are chemically and mechanically pretty stable and they exhibit para- to ferroelectric phase transition at or above room temperature. Continued interest in these compounds has led to a wide variety of theoretical and experimental work, specially on lattice vibrations. A less common approach has been those based on electronic structure calculations [6]. Michel-Calendini and Mesnard [7]-[8] have reported band structure of  $BaTiO_3$  within a linear combination of atomic orbitals (LCAO) method with empirical off-diagonal integrals. The pioneering work on  $SrTiO_3$  was that of Kahn and Leyendecker [9]. This was followed by an Augmented Plane Wave (APW) calculation by Matheiss [10] and a self-consistent tight-binding calculation by Soules *et al* [11]. However, Battaye *et al* [12] have compared experimental valence-band spectra with these early theoretical predictions and have concluded that the agreement

was not satisfying. Pertosa and Michel-Calendini [13] carried out a modified tight-binding calculation on  $BaTiO_3$  and  $SrTiO_3$  and compared their results with X-ray photoelectron spectra. These authors introduced inner orbital interactions. Perkins and Winter [14] have carried out LCAO calculations on the band structure of  $SrTiO_3$ . There have been several all-electron, full-potential linearized augmented plane waves (FP-LAPW) studies of the titanates in recent times [17]-[19]. In addition ultrasoft-pseudopotential, local density approximation (LDA) based studies on perovskites have been carried out by King-Smith and Vanderbilt [20]. In comparison, electronic structure calculations on  $CaTiO_3$  have been fewer. Ueda and coworkers [25]-[26] have used the first-principles tight-binding method to study  $CaTiO_3$ .

We shall show that for all the three compounds the transition rate, defined by us, is strongly energy and frequency dependent, i.e. it depends upon the energy of both the initial and the final states. We shall compare the theoretical results with experiment.

## 2. Methodology

In recent years a number of methods have been proposed for calculating optical properties within the framework of the LMTO [27]-[32] for both metals and semiconductors. We shall present here a gauge-independent formalism, following the ideas of Hobbs *et al* [32]. Since our final aim is to use the augmented space recursion method (ASR) [1]-[5] and study the optical properties of random systems, we shall modify the reciprocal space formulation and obtain an expression in which all states are labelled by their energy and the optical conductivity is expressed as a convolution of the energy resolved joint density of states and an energy-frequency dependent transition matrix. This formulation will then be directly generalized within the ASR.

The Hamiltonian describing the effect of a radiation field on the electronic states of a solid is given by :

$$H = \sum_{i=1}^N \left\{ \frac{1}{2m_e} \left( \mathbf{p}_i + \frac{e}{c} \mathbf{A}(\mathbf{r}_i, t) \right)^2 + V(\mathbf{r}_i) + e\Phi(\mathbf{r}_i, t) \right\}$$

Here  $e$  is the magnitude of electronic charge,  $m_e$  the electronic mass,  $c$  is the velocity of light and  $\hbar$  is the Planck's constant.  $\mathbf{A}(\mathbf{r}_i, t)$  and  $\Phi(\mathbf{r}_i, t)$  are the vector and scalar potentials seen by the  $i$ -th electron because of the radiation field. There are  $N$  electrons labelled by  $i$ . The potential  $V(\mathbf{r}_i)$  experienced by the electrons is expressed as an effective independent electron approximation within the LDA of the density functional theory (DFT). For not too large external optical fields, neglecting terms of the order of  $O(|\mathbf{A}|^2)$ , the Hamiltonian reduces to :

$$H = \sum_{i=1}^N \left\{ \frac{1}{2m_e} \mathbf{p}_i^2 + V(\mathbf{r}_i) + \frac{1}{c} \mathbf{j}_i \cdot \mathbf{A}(\mathbf{r}_i, t) \right\} \quad (1)$$

Here  $\mathbf{j}_i = (e/m) \mathbf{p}_i$  is the current operator. We work in the Coulomb gauge where  $\nabla \cdot \mathbf{A}(\mathbf{r}_i, t) = 0$  and  $\Phi(\mathbf{r}_i, t) = 0$ , so that the electric field

$$\mathbf{E}(\mathbf{r}_i, t) = -\frac{\partial \mathbf{A}(\mathbf{r}_i, t)}{\partial t}$$

In choosing the above equation we have ignored the response of the system. The local electric field is the external field due to the incident radiation as well as the internal field due to the polarization of the medium. Such local field corrections are important for insulators. We intend, as is customary, to introduce the local field corrections as well as corrections due to the Coulomb hole in our final GW calculations, for which these single-particle picture will form the zeroth starting point.

The Kubo formula then relates the linear current response to the radiation field :

$$\langle j_\mu(t) \rangle = \sum_\nu \int_{-\infty}^{\infty} dt' \chi_{\mu\nu}(t-t') A_\nu(t')$$

The generalized susceptibility is given by :

$$\chi_{\mu\nu}(\tau) = i\Theta(\tau) \langle \phi_0 | [j_\mu(\tau), j_\nu(0)] | \phi_0 \rangle$$

where,  $\tau = t - t'$  and  $\Theta(\tau)$  is the Heaviside step function,

$$\Theta(\tau) = \begin{cases} 1 & \text{if } \tau > 0 \\ 0 & \text{if } \tau \leq 0 \end{cases}$$

$|\phi_0\rangle$  is the ground state of the unperturbed system, that is the solid in the absence of the radiation field. In the absence of the radiation field, there is no photocurrent, i.e.  $\langle \phi_0 | j_\mu | \phi_0 \rangle = 0$ . The fluctuation-dissipation theorem relates the imaginary part of the generalized susceptibility to the correlation function as follows :

$$\chi''_{\mu\nu}(\omega) = \frac{1}{2} (1 - e^{-\beta\omega}) S_{\mu\nu}(\omega) \quad (2)$$

where,

$$\beta = \frac{1}{k_B T} \quad \text{where } k_B \text{ is the Boltzmann constant and } T \text{ the temperature}$$

and

$$\chi''_{\mu\nu}(\omega) = \Im m \int_{-\infty}^{\infty} dt e^{iz\tau} \chi_{\mu\nu}(\tau) \quad z = \omega + i0^+$$

and,

$$S_{\mu\nu}(\omega) = \Im m \int_{-\infty}^{\infty} dt e^{iz\tau} \langle \phi_0 | j_\mu(\tau) j_\nu(0) | \phi_0 \rangle \quad z = \omega + i0^+$$

An expression for the correlation function, can be obtained via the Kubo-Greenwood expression,

$$S(\omega) = \frac{\pi}{3} \sum_i \sum_f \sum_\mu \langle \phi_i | j_\mu | \phi_f \rangle \cdot \langle \phi_f | j_\mu | \phi_i \rangle \delta(E_f - E_i - \hbar\omega) \quad (3)$$

We have assumed isotropy of the response so that the tensor  $S_{\mu\nu}$  is diagonal and we have defined  $S(\omega)$  as the direction averaged quantity  $\frac{1}{3} \sum_\mu S_{\mu\mu}(\omega)$ . The  $|\{\phi_i\}\rangle$  are the occupied ‘initial’ single electronic states in the ground state while  $|\{\phi_f\}\rangle$  are the unoccupied single electron ‘final’ excited states in the LDA description.

The imaginary part of the dielectric function is related to the above :

$$\epsilon_2(\omega) = \frac{1}{\pi^2 \omega^2} S(\omega) \quad (4)$$

We may obtain the real part of the dielectric function  $\epsilon_1(\omega)$  from a Kramers-Krönig relationship.

For crystalline semi-conductors the equation (3) may be rewritten as follows :

$$S(\omega) = \frac{\pi}{3} \sum_j \sum_{j'} \int_{BZ} \frac{d^3\mathbf{k}}{8\pi^3} |\langle \Phi_{j'\mathbf{k}} | \mathbf{j} | \Phi_{j\mathbf{k}} \rangle|^2 \delta(E_{j'}(\mathbf{k}) - E_j(\mathbf{k}) - \hbar\omega) \quad (5)$$

Here  $j$  and  $j'$  refer to band labels :  $j$  for the occupied valence bands and  $j'$  the unoccupied conduction bands at T=0 K. The  $\mathbf{k}$  is the quantum label associated with the Bloch Theorem. For disordered materials, the Bloch Theorem fails and the expression (5) can no longer be used. Our first aim will be to obtain an alternative expression where the quantum states are directly labelled by energy and frequency, rather than by the ‘band’ and ‘crystal momentum’ indices. For this, let us examine the following expressions :

$$n(E) = \sum_j \int_{BZ} \frac{d^3\mathbf{k}}{8\pi^3} \delta(E_j(\mathbf{k}) - E) \quad (6)$$

$$J(E, \omega) = \sum_j^{occ} \sum_{j'}^{unocc} \int_{BZ} \frac{d^3\mathbf{k}}{8\pi^3} \delta(E_j(\mathbf{k}) - E) \delta(E_{j'}(\mathbf{k}) - E - \hbar\omega) \quad (7)$$

In the equation (6), the right hand side picks up a factor of 1 whenever a quantum state, labelled by  $\{\mathbf{k}, j\}$  falls in the range  $E, E+\delta E$ . The left-hand side, therefore, is the *density of states* arising from the bands labelled  $j$ .

In the equation (7), the right-hand side picks up a factor of 1 whenever a quantum state in the filled bands labelled  $j$  falls in the range  $E, E+\delta E$  and *simultaneously* a quantum state in the unfilled bands labelled  $j'$  falls in the range  $E+\omega, E+\omega+\delta E$ . The left-hand side is then the *energy resolved joint density of states* :

$$J(E, \omega) = n_v(E) n_c(E + \hbar\omega) \quad (8)$$

We shall define the energy-frequency labelled *Transition rate* as :

$$T(E, \omega) = \frac{\sum_j \sum_{j'} \int_{BZ} \frac{d^3 \mathbf{k}}{8\pi^3} T^{jj'}(\mathbf{k}) \delta(E_j(\mathbf{k}) - E) \delta(E_{j'}(\mathbf{k}) - E - \hbar\omega)}{\sum_j \sum_{j'} \int_{BZ} \frac{d^3 \mathbf{k}}{8\pi^3} \delta(E_j(\mathbf{k}) - E) \delta(E_{j'}(\mathbf{k}) - E - \hbar\omega)} \quad (9)$$

Where,

$$T^{jj'}(\mathbf{k}) = \sum_{\mu} \left| \langle \Phi_{j'\mathbf{k}} | j_{\mu} | \Phi_{j\mathbf{k}} \rangle \right|^2$$

The expression for  $S(\omega)$  from equation (5) then becomes,

$$S(\omega) = (\pi/3) \int dE T(E, \omega) J(E, \omega) \quad (10)$$

Many earlier workers argued that the transition matrix element is weakly dependent on both  $E$  and  $\omega$ . They then assumed it to be constant  $T_0$  and obtained a simple expression for the correlation function :

$$S_0(\omega) = (\pi/3) T_0 \int dE J(E, \omega) \quad (11)$$

We shall investigate the validity of this approximation for the systems under study in this communication. Let us first get an expression for the equation (10) within the TB-LMTO formalism of [21]-[23] : The basis of the LMTO starts from the minimal muffin-tin orbital basis set of a KKR formalism and then linearizes it by expanding around a ‘nodal’ energy point  $E_{\nu\ell}^{\alpha}$ . The wave-function is then expanded in this basis :

$$\Phi_{j\mathbf{k}}(\mathbf{r}) = \sum_L \sum_{\alpha} c_{L\alpha}^{j\mathbf{k}} \left[ \phi_{\nu L}^{\alpha}(\mathbf{r}) + \sum_{L'} \sum_{\alpha'} h_{LL'}^{\alpha\alpha'}(\mathbf{k}) \dot{\phi}_{\nu L'}^{\alpha'}(\mathbf{r}) \right]$$

where,  $L$  is the composite angular momentum index  $(\ell, m)$ ,  $j$  is the band index and  $\alpha$  labels the atom in the unit cell.

and,

$$\begin{aligned} \phi_{\nu L}^{\alpha}(\mathbf{r}) &= i^{\ell} Y_L(\hat{r}) \phi_{\ell}^{\alpha}(r, E_{\nu\ell}^{\alpha}) \\ \dot{\phi}_{\nu L}^{\alpha}(\mathbf{r}) &= i^{\ell} Y_L(\hat{r}) \frac{\partial \phi_{\ell}^{\alpha}(r, E_{\nu\ell}^{\alpha})}{\partial E} \\ h_{LL'}^{\alpha\alpha'}(\mathbf{k}) &= (C_L^{\alpha} - E_{\nu\ell}^{\alpha}) \delta_{LL'} \delta_{\alpha\alpha'} + \sqrt{\Delta_L^{\alpha}} S_{LL'}^{\alpha\alpha'}(\mathbf{k}) \sqrt{\Delta_{L'}^{\alpha'}} \end{aligned}$$

$C_L^\alpha$  and  $\Delta_L^\alpha$  are TB-LMTO potential parameters and  $S_{LL'}^{\alpha\alpha'}(\mathbf{k})$  is the structure matrix. These terms are standard for the LMTO formulation and the reader is referred to the citation [21] for greater detail. The TB-LMTO secular equation provides the expansion coefficients  $c_{L\alpha}^{j\mathbf{k}}$  via :

$$\sum_{L'} \sum_{\alpha'} \left[ h_{LL'}^{\alpha\alpha'}(\mathbf{k}) + (E_{\nu\ell}^\alpha - E^{j\mathbf{k}}) \delta_{LL'} \delta_{\alpha\alpha'} \right] c_{L'\alpha'}^{j\mathbf{k}} = 0 \quad (12)$$

We may now immediately write an expression for the matrix element of the current operator as in equation (9) :

$$\begin{aligned} \langle \Phi_{j'\mathbf{k}}(\mathbf{r}) | \mathbf{j} | \Phi_{j\mathbf{k}}(\mathbf{r}) \rangle &= \sum_{LL'} \sum_{\alpha} \bar{c}_{L'\alpha}^{j'\mathbf{k}} c_{L\alpha}^{j\mathbf{k}} \left\{ \langle \phi_{\nu L'}^\alpha(\mathbf{r}) | \mathbf{j} | \phi_{\nu L}^\alpha(\mathbf{r}) \rangle \dots \right. \\ &\dots + (E^{j\mathbf{k}} - E_{\nu\ell}^\alpha) \langle \phi_{\nu L'}^\alpha(\mathbf{r}) | \mathbf{j} | \dot{\phi}_{\nu L}^\alpha(\mathbf{r}) \rangle \dots \\ &\dots + (E^{j'\mathbf{k}} - E_{\nu\ell'}^\alpha) \langle \dot{\phi}_{\nu L'}^\alpha(\mathbf{r}) | \mathbf{j} | \phi_{\nu L}^\alpha(\mathbf{r}) \rangle \dots \\ &\left. \dots + (E^{j\mathbf{k}} - E_{\nu\ell}^\alpha) (E^{j'\mathbf{k}} - E_{\nu\ell'}^\alpha) \langle \dot{\phi}_{\nu L'}^\alpha(\mathbf{r}) | \mathbf{j} | \dot{\phi}_{\nu L}^\alpha(\mathbf{r}) \rangle \right\} \end{aligned} \quad (13)$$

We shall now obtain expressions for the right-hand terms by noting the following :

$$\begin{aligned} \mathbf{j} &= e \frac{d\mathbf{r}}{dt} = \frac{e}{i\hbar} [\mathbf{r}, H] \\ H \phi_{\nu L}^\alpha(\mathbf{r}) &= E_{\nu\ell}^\alpha \phi_{\nu L}^\alpha(\mathbf{r}) \\ H \dot{\phi}_{\nu L}^\alpha(\mathbf{r}) &= \dot{\phi}_{\nu L}^\alpha(\mathbf{r}) + E_{\nu\ell}^\alpha \dot{\phi}_{\nu L}^\alpha(\mathbf{r}) \end{aligned} \quad (14)$$

We can write,

$$\mathbf{r} = (2\pi/3)^{1/2} r \left[ (Y_{1,-1} - Y_{1,1}) \hat{\mathbf{i}} + i(Y_{1,-1} + Y_{1,1}) \hat{\mathbf{j}} + 2^{1/2} Y_{1,0} \hat{\mathbf{k}} \right]$$

Using the above two equations we get,

$$\int \phi_{\nu L'}^\alpha(\mathbf{r})^* \mathbf{r} H \phi_{\nu L}^\alpha(\mathbf{r}) d^3\mathbf{r} = i^{\ell-\ell'} E_{\nu\ell}^\alpha \mathbf{\Gamma}_{LL'} \int_0^{s_\alpha} \phi_{\nu\ell'}^\alpha(r) \phi_{\nu\ell}^\alpha(r) r^3 dr \quad (15)$$

where,  $s_\alpha$  is the atomic sphere radius of the  $\alpha$ -th atom in the unit cell and  $\mathbf{\Gamma}_{LL'}$  is a combination of Gaunt coefficients [32] :

$$\mathbf{\Gamma}_{LL'} = \sqrt{\frac{2\pi}{3}} \left[ (G_{\ell',1,\ell}^{m',-1,m} - G_{\ell',1,\ell}^{m',1,m}) \hat{\mathbf{i}} + i(G_{\ell',1,\ell}^{m',-1,m} + G_{\ell',1,\ell}^{m',1,m}) \hat{\mathbf{j}} + \sqrt{2} G_{\ell',1,\ell}^{m',0,m} \hat{\mathbf{k}} \right]$$

In order to obtain  $\int \phi_{\nu L'}^\alpha(\mathbf{r})^* H \mathbf{r} \phi_{\nu L}^\alpha(\mathbf{r}) d^3\mathbf{r}$ , we note that  $H = (\hbar^2/2m_e)\nabla^2 + V(\mathbf{r})$  so that using the Green's second identity we can obtain,

$$\int \phi_{\nu L'}^\alpha(\mathbf{r})^* H \mathbf{r} \phi_{\nu L}^\alpha(\mathbf{r}) d^3 \mathbf{r} = i^{\ell-\ell'} \Gamma_{LL'} \left\{ E_{\nu\ell'}^\alpha \int_0^{s_\alpha} \phi_{\nu\ell'}^\alpha(r) \phi_{\nu\ell}^\alpha(r) r^3 dr \dots \right. \\ \left. \dots + (\hbar^2/2m_e) s_\alpha^2 \phi_{\nu\ell}^\alpha(s_\alpha) \phi_{\nu\ell'}^\alpha(s_\alpha) (D_{\nu\ell'}^\alpha - D_{\nu\ell}^\alpha - 1) \right\} \quad (16)$$

$D_{\nu\ell}^\alpha$  is the logarithmic derivative of  $\phi_{\nu\ell}^\alpha(r)$  at  $r = s_\alpha$  and are obtained as parameters in the TB-LMTO routines. We define the following integrals :

$$\int_0^{s_\alpha} \phi_{\nu\ell'}^\alpha(r) \phi_{\nu\ell}^\alpha(r) r^3 dr = I_{\ell\ell'}^\alpha \\ \int_0^{s_\alpha} \phi_{\nu\ell'}^\alpha(r) \dot{\phi}_{\nu\ell}^\alpha(r) r^3 dr = J_{\ell\ell'}^\alpha \\ \int_0^{s_\alpha} \dot{\phi}_{\nu\ell'}^\alpha(r) \dot{\phi}_{\nu\ell}^\alpha(r) r^3 dr = K_{\ell\ell'}^\alpha$$

call,

$$(\hbar^2/2m_e) s_\alpha^2 (D_{\nu\ell}^\alpha - D_{\nu\ell'}^\alpha - 1) = \mathcal{D}_{\ell\ell'}^\alpha$$

Then the matrix elements for the current operator becomes :

$$\mathcal{I}_{LL',\mu}^{(1),\alpha} = \langle \phi_{\nu L'}^\alpha(\mathbf{r}) | j_\mu | \phi_{\nu L}^\alpha(\mathbf{r}) \rangle = \frac{i^{\ell-\ell'-1}}{\hbar} \Gamma_{LL'}^\mu \left[ \tilde{E} I_{\ell\ell'}^\alpha - \mathcal{D}_{\ell\ell'}^\alpha \phi_{\nu\ell}^\alpha(s_\alpha) \phi_{\nu\ell'}^\alpha(s_\alpha) \right] \\ \mathcal{I}_{LL',\mu}^{(2),\alpha} = \langle \phi_{\nu L'}^\alpha(\mathbf{r}) | j_\mu | \dot{\phi}_{\nu L}^\alpha(\mathbf{r}) \rangle = \frac{i^{\ell-\ell'-1}}{\hbar} \Gamma_{LL'}^\mu \left[ \tilde{E} J_{\ell\ell'}^\alpha + I_{\ell\ell'}^\alpha - \mathcal{D}_{\ell\ell'}^\alpha \dot{\phi}_{\nu\ell}^\alpha(s_\alpha) \phi_{\nu\ell'}^\alpha(s_\alpha) \right] \\ \mathcal{I}_{LL',\mu}^{(3),\alpha} = \langle \dot{\phi}_{\nu L'}^\alpha(\mathbf{r}) | j_\mu | \phi_{\nu L}^\alpha(\mathbf{r}) \rangle = \frac{i^{\ell-\ell'-1}}{\hbar} \Gamma_{LL'}^\mu \left[ \tilde{E} J_{\ell\ell'}^\alpha - I_{\ell\ell'}^\alpha - \mathcal{D}_{\ell\ell'}^\alpha \phi_{\nu\ell}^\alpha(s_\alpha) \dot{\phi}_{\nu\ell'}^\alpha(s_\alpha) \right] \\ \mathcal{I}_{LL',\mu}^{(4),\alpha} = \langle \dot{\phi}_{\nu L'}^\alpha(\mathbf{r}) | j_\mu | \dot{\phi}_{\nu L}^\alpha(\mathbf{r}) \rangle = \frac{i^{\ell-\ell'-1}}{\hbar} \Gamma_{LL'}^\mu \left[ \tilde{E} K_{\ell\ell'}^\alpha + J_{\ell\ell'}^\alpha - J_{\ell\ell'}^\alpha \dots \right. \\ \left. \dots - \mathcal{D}_{\ell\ell'}^\alpha \dot{\phi}_{\nu\ell}^\alpha(s_\alpha) \dot{\phi}_{\nu\ell'}^\alpha(s_\alpha) \right] \quad (17)$$

where,  $\tilde{E} = E_{\nu\ell}^\alpha - E_{\nu\ell'}^\alpha$

The transition term  $T^{jj'}(\mathbf{k})$  has to be written in terms of the normalized wavefunction.

The normalizing factor for the wavefunctions are obtained from :

$$N_{\mathbf{k}}^j = \int d^3 \mathbf{r} \Phi_{j\mathbf{k}}^*(\mathbf{r}) \Phi_{j\mathbf{k}}(\mathbf{r}) \\ = \sum_L \sum_\alpha |\bar{c}_{L\alpha}^{j\mathbf{k}}|^2 \left\{ \mathcal{J}_{L\alpha}^{(1)} + 2(E^{j\mathbf{k}} - E_{\nu\ell}^\alpha) \mathcal{J}_{L\alpha}^{(2)} + (E^{j\mathbf{k}} - E_{\nu\ell}^\alpha)^2 \mathcal{J}_{L\alpha}^{(3)} \right\} \quad (18)$$



where,

$$\begin{aligned}\mathcal{J}_{L\alpha}^{(1)} &= \int_0^{s_\alpha} |\phi_{\nu L}^\alpha(r)|^2 r^2 dr \\ \mathcal{J}_{L\alpha}^{(2)} &= \int_0^{s_\alpha} \phi_{\nu L}^\alpha(r)^* \dot{\phi}_{\nu L}^\alpha(r) r^2 dr \\ \mathcal{J}_{L\alpha}^{(3)} &= \int_0^{s_\alpha} |\dot{\phi}_{\nu L}^\alpha(r)|^2 r^2 dr\end{aligned}$$

Using the secular equation (12), the expression for the transition term becomes,

$$\begin{aligned}T^{jj'}(\mathbf{k}) &= \left(N_{\mathbf{k}}^j N_{\mathbf{k}}^{j'}\right)^{-1/2} \left| \sum_{\mu} \sum_{LL'} \sum_{\alpha} \bar{c}_{L'\alpha}^{j'\mathbf{k}} c_{L\alpha}^{j\mathbf{k}} \left\{ \mathcal{I}_{LL',\mu}^{(1)\alpha} + (E^{j\mathbf{k}} - E_{\nu\ell}^\alpha) \mathcal{I}_{LL',\mu}^{(2)\alpha} \dots \right. \right. \\ &\quad \left. \left. \dots + (E^{j'\mathbf{k}} - E_{\nu\ell'}^\alpha) \mathcal{I}_{LL',\mu}^{(3)\alpha} + (E^{j\mathbf{k}} - E_{\nu\ell}^\alpha)(E^{j'\mathbf{k}} - E_{\nu\ell'}^\alpha) \mathcal{I}_{LL',\mu}^{(4)\alpha} \right\} \right|^2\end{aligned}\tag{19}$$

The equation (10) provides an expression for the optical conductivity where both the transition matrix and the energy resolved joint density of states are expressed as functions of energy and frequency. As we shall show in a subsequent communication, that within the ASR formalism, this is the form in which the information about the constituents are input and the configuration averaged correlation function for the alloy may be expressed as :

$$\ll S(\omega) \gg = (\pi/3) \int dE T^{eff}(E, \omega) \ll J(E, \omega) \gg\tag{20}$$

where,

$$\ll J(E, \omega) \gg = \ll n_v(E) \gg \ll n_c(E + \omega) \gg \left[ 1 + \Lambda(E, \omega) \ll J(E, \omega) \gg \right]$$

and,

$$T^{eff}(E, \omega) = \ll T(E, \omega) \gg + \delta T(E, \omega, \Sigma(E, \omega))$$

where,  $\Sigma(E, \omega)$  is the self-energy due to disorder scattering and  $\Lambda(E, \omega)$  the corresponding vertex correction. The details of the derivation will be communicated in a subsequent paper [24].

### 3. Computational Details and Results

The primitive cell for the ideal perovskite structure  $ABC_3$  is illustrated in figure 1 (a). For the class of compounds we are interested in, the generic chemical formula is  $ABO_3$ .  $A$  is a mono or divalent cation,  $B$  is a tetra or penta-valent metal. In the

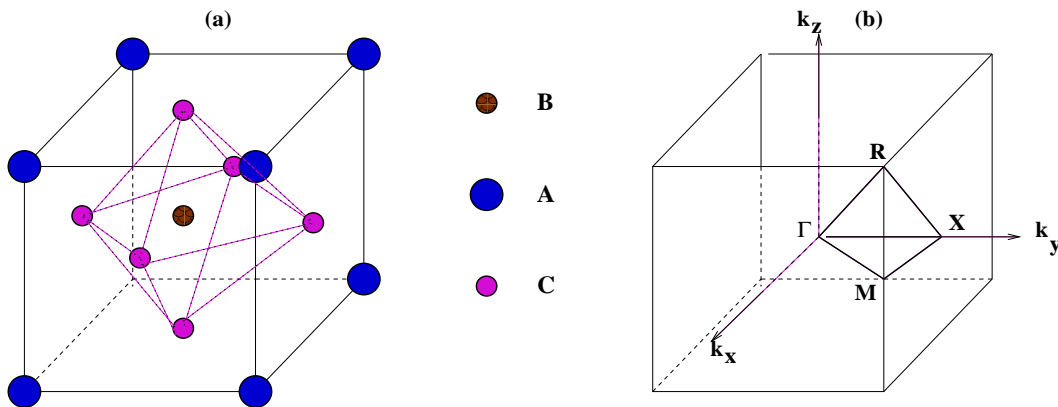


**Figure 1.** (a) Cubic unit cell for a perovskite  $ABC_3$ . (b) The Brilluoin zone for the cubic phase

paraelectric phase there is full cubic symmetry. It can be thought of as lattice of corner sharing oxygen octahedra with inter-penetrating simple cubic lattices of  $A$  and  $B$ . The  $B$  cations sit in the centre of the octahedral O cage, while the  $A$  metal ions sit in the 12-fold coordinated sites between the octahedra. In our case the body centre position is occupied by the Ti atom, the edges by alkaline earth atoms and the face centres by O atoms. The space group is  $O_h^1$  and the corresponding Brilluoin zone is shown in figure 1 (b). Both the  $A$  and  $B$  atoms are situated at sites with full cubic ( $O_h$ ) point symmetry, while the O atoms have tetragonal ( $D_{4h}$ ) symmetry.

The electronic configuration of the alkali earth atoms are as follows :

Atom	Deep Core	Shallow Core	Valence	Unoccupied
Ca	$1s^2 2s^2 2p^6 3s^2 3p^6$	-	$4s^2$	$3d 4p$
Sr	$1s^2 2s^2 2p^6 3s^2 3p^6 3d^{10} 4s^2$	$4p^6$	$5s^2$	$4d 5p 4f$
Ba	$1s^2 2s^2 2p^6 3s^2 3p^6 3d^{10} 4s^2 4p^6 4d^{10} 5s^2$	$5p^6$	$6s^2$	$5d 6p 4f$
Ti	$1s^2 2s^2 2p^6 3s^2 3p^6$	-	$3d^2 4s^2$	$4p$
O	$1s^2$	-	$2s^2 2p^4$	$3s 3d$

Since we wish to take into account the shallow core states, to include the transitions from these to the conduction band at large enough optical frequencies, the energy range is about 40 eV (3 Ryd) and the single panel LMTO cannot be made to be accurate over this range, we have carried out a two panel calculation, with the  $E_{\nu\ell}^\alpha$  lying in the lower energy range in one panel and in the upper energy range in the other. The minimal basis set used in the two panels are the following :

$CaTiO_3$	
Lower Panel	Ca 4s 4p 3d, Ti 4s 4p 3d, O 2s 2p (3d)
Upper Panel	Ca 4s 4p 3d, Ti 4s 4p 3d, O 3s 2p (3d)
$SrTiO_3$	
Lower Panel	Sr 5s 4p 4d (4f), Ti 4s 4p 3d, O 2s 2p (3d)
Upper Panel	Sr 5s 5p 4d (4f), Ti 4s 4p 3d, O 3s 2p (3d)
$BaTiO_3$	
Lower Panel	Ba 6s 5p 5d (4f), Ti 4s 4p 3d, O 2s 2p (3d)
Upper Panel	Ba 6s 6p 3d (4f), Ti 4s 4p 3d, O 3s 2p (3d)

The states in parentheses are unfilled states which have been downfolded in our calculations. The figure 2 shows the band structure of the three titanates.

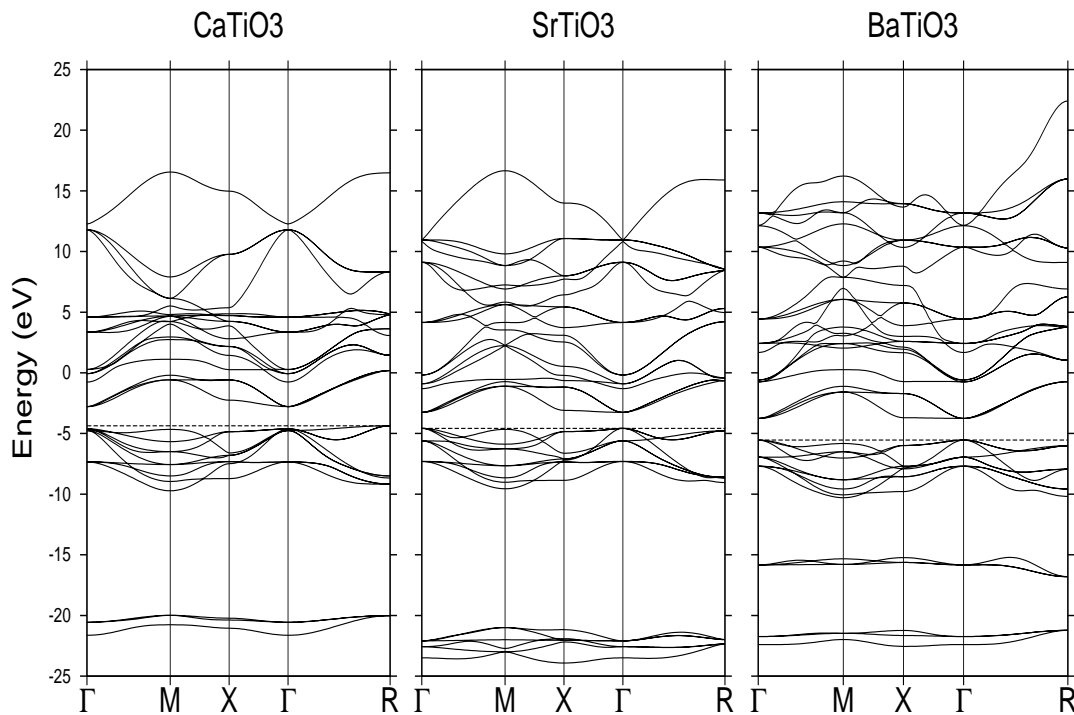


**Figure 2.** Band structures of  $CaTiO_3$ ,  $SrTiO_3$  and  $BaTiO_3$  (No scissors operation has been carried out in these calculations)

Let us first look at the leftmost figure for  $CaTiO_3$ . The Ca 3p core level lies around  $-27$  eV and not shown in this figure. The narrow band around  $-20$  eV is the O 2s band. The nine valence bands just below the Fermi level are derived from hybridized Ti 4s and O 2p. An indirect band gap appears between the valence band top at the R point and the conduction band minimum at the  $\Gamma$  point.  $CaTiO_3$  shows an indirect band gap ( $\Gamma$ -R) of 1.6 eV, in the absence of the scissors operation. The experimentally

reported indirect gap is 3.5 eV [25]. This discrepancy is characteristic of the Local density Approximation (LDA) upon which the TB-LMTO is based. In the conduction band region we have bands originating from (in ascending order of energy) Ti  $3d t_{2g}$  triplet, a singlet arising from Ca  $4s$  and a doublet from Ti  $3d e_g$ . Then comes the bands which originate from the Ca  $3d e_g$  doublet and the Ca  $3d t_{2g}$  triplet. Finally we have the Ti  $4p$  and Ca  $4p$  based bands and finally the band based on Ca  $4s$ . We note that for  $CaTiO_3$ , Ca and Ti  $3d$  based bands overlap and hybridize in the conduction region.

For  $SrTiO_3$ , in the lower panel, the Sr  $4p$  level now sits almost atop the O  $2s$  band, giving rise to a rather broad (as compared to  $CaTiO_3$ )  $s-p$  hybridized band just below  $-20$  eV. The subsequent analysis of the bands is rather similar to  $CaTiO_3$ . However, the band gap is now direct and  $\sim 1.4$  eV. Earlier band structure calculations of Mo *et al* [33] and Kimura *et al* [34] yield indirect band gaps of  $\sim 1.45$  eV and  $\sim 1.79$  eV respectively. The experimental direct band gap is around 3.2 eV.

For  $BaTiO_3$ , in the lower panel, the Ba  $5p$  shallow core level now crosses and lies above the O  $2s$  band. The band gap is direct and  $\sim 1.2$  eV. The band structure is almost identical to the pseudopotential calculations of King-Smith and Vanderbilt [20], whose band gap was also direct and  $\sim 1.8$  eV. The experimental band gap turns out to be  $\sim 3.2$  eV [35].

For all three compounds, our calculations show a characteristic flatness of the lowest conduction band along  $\Gamma$  to X. This agrees with earlier works of Cardona [36], Matheiss [10], Harrison [37], Wolfram and Ellialtıođlu [38] and King-Smith and Vanderbilt [20]. This observed flatness is related to certain unusual features in the density of states and optical conductivity, which appear to be characteristic of pseudo- two-dimensional systems.

Figure 3 shows the densities of states for the three titanates. The densities of states reflect the detailed band structure we have described above. Earlier works on the density of states were based on different methods. Michel-Calendini and Mesnard [7, 8] and Pertosa and Michel-Calendini [13] have used parameterized tight-binding and adjusted LCAO based methods for  $BaTiO_3$ . Their density of states is in agreement with ours, with the band gap difference characteristic of LSDA methods like the TB-LMTO. Similarly, Matheiss [10] used the LCAO and Perkins and Winter [14] used the extended Húkel basis for  $SrTiO_3$ . Again their band structures and densities of states are in agreement with ours, with the exception of the band gap. Even earlier works on  $SrTiO_3$  by Zook and Castelman [15] and Soules *et al* [16] also show reasonable agreement. For  $CaTiO_3$  we may compare our results with those of Ueda *et al* [25], which agree reasonably well with our results.

Figure 4 displays the transition rates  $T(E, \omega)$  for the three titanates, shown here as functions of the initial energy of the excited electron and the incident photon energy (frequency). It is clear from the figure that the transition rate is strongly dependent on the energy-frequency variables for all the three compounds. The usual assumption of a

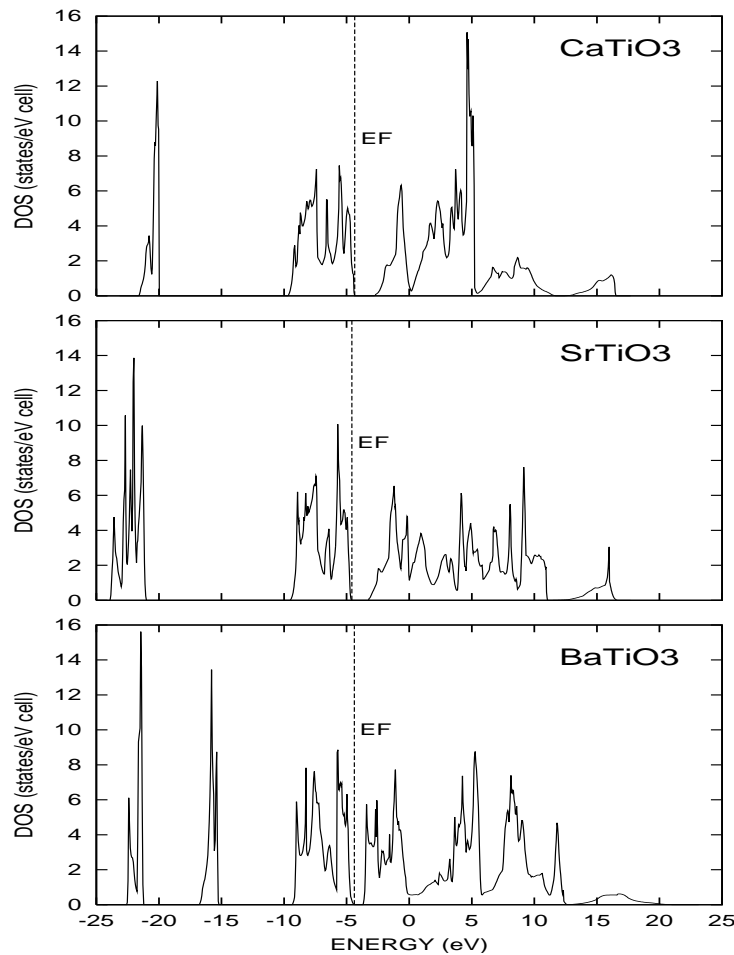


**Figure 3.** Densities of states for the three perovskite titanates

transition matrix, weakly dependent on energy and frequency is certainly not valid in any of the three cases [39]-[41].

In figure 5 we compare the imaginary part of the dielectric function with the scaled joint-density of states/ $\omega^2$ . If the transition rate were independent of energy and frequency, they should be the same. The behaviour of the two are similar, but the relative weights of the structures across the frequency range are clear indications of the energy-frequency dependence of the transition rates.

*CaTiO<sub>3</sub>* :

The effect of energy-frequency dependence of the transition rate has a large effect for the optical properties of *CaTiO<sub>3</sub>*. If we compare the results reported in [41] with our figure 6 we note that although in the earlier work the joint density of states does reproduce the peaks at lower frequencies, the relative heights are not replicated. Looking at the lower panel of the figure, we may assign the peak at 4.5 eV to the transitions :

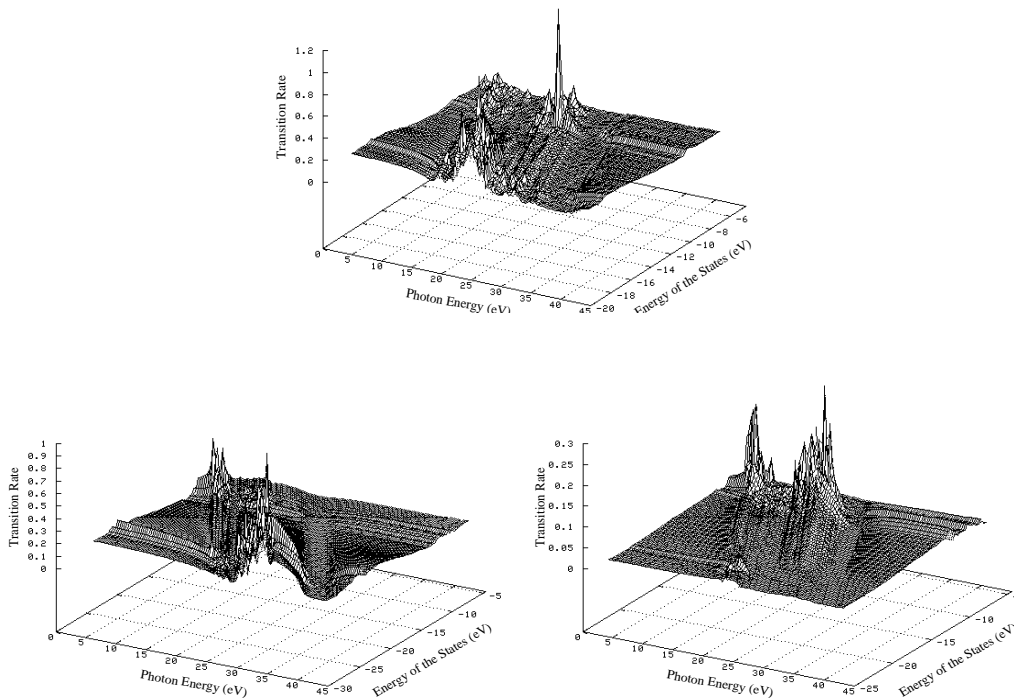


**Figure 4.** Transition rates for the three perovskite titanates shown as functions of initial energies and incident photon energies.  $BaTiO_3$  (top),  $SrTiO_3$  (left-bottom) and  $CaTiO_3$  (right-bottom)

$O\ 2p \rightarrow Ti\ 3d-t_{2g}$  at the R and X-points. The next and highest peak arises because of the nearby two unresolved peaks due to the transitions :  $O\ 2p \rightarrow Ca\ 4s$  at the M-point (at 6.3 eV) and  $O\ 2p \rightarrow Ca\ 3d-e_g$  at the M-point (at 6.8 eV). The third peak at 7.5 eV may be assigned to the transitions :  $O\ 2p \rightarrow Ti\ 3d-t_{2g}$  at the R-point and  $O\ 2p \rightarrow Ca\ 3d-e_g$  at the X-point. At higher frequencies, the theory does not tally well with experiment. The peak at 10 eV is not reproduced except as a shoulder. The real part of the dielectric function  $\epsilon_1(\omega)$  is obtained by a Kramers-Krönig transformation from the imaginary part. This is shown in the top panel of figure 6. The discrepancies at high frequencies could be due to the fact that in the scissors type approach we have provided a rigid shift to the conduction bands. In a full fledged many-body GW technique, which is our ultimate aim to produce, the shift, due to the self-energy will turn out to be energy (frequency) dependent.

$SrTiO_3$  :

Let us now examine the figure 7. As in the case of  $CaTiO_3$  , here too, the effect of energy-frequency dependence of the transition rate reproduces the correct relative

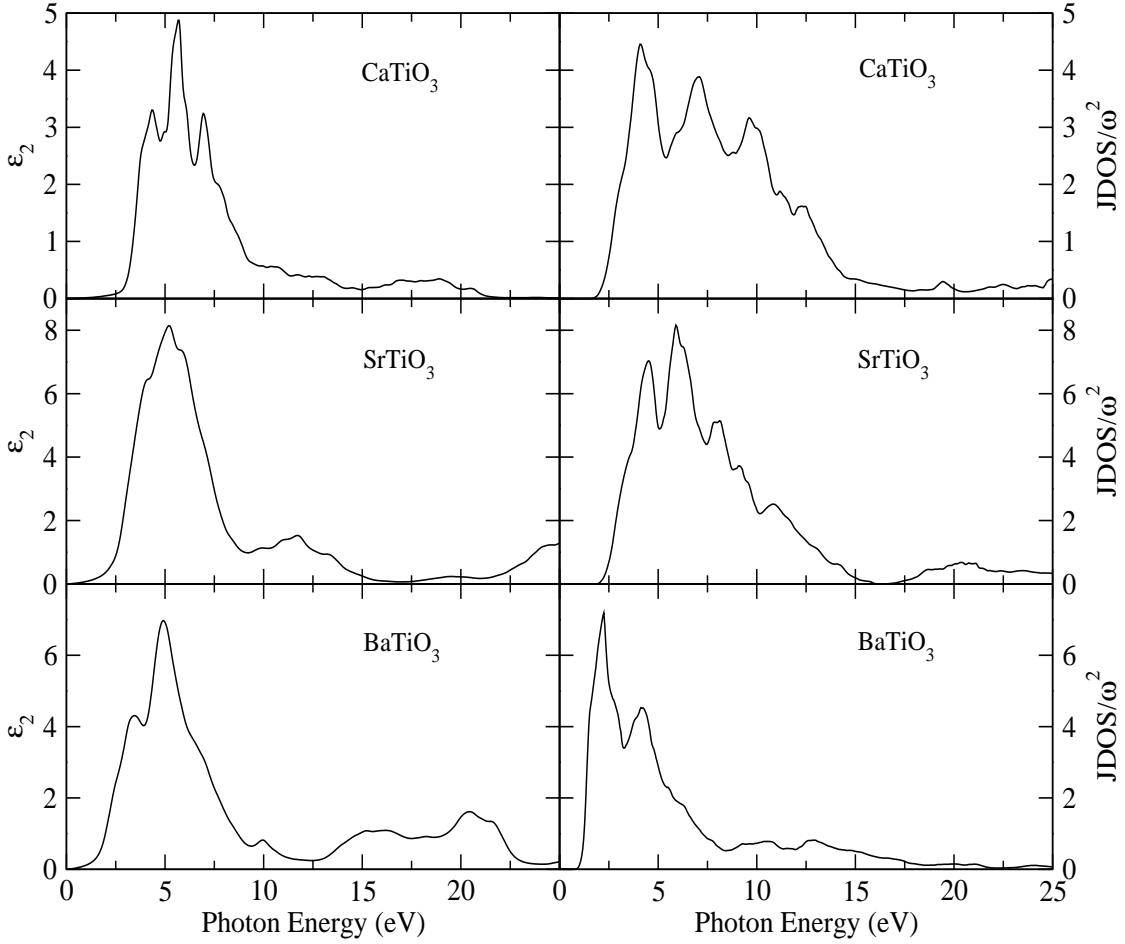


**Figure 5.** Comparison of the calculated imaginary part of the dielectric function ( $\epsilon_2$ ) (left) for the three perovskite titanates with the same function calculated considering transition rate is constant (right).

heights of the peaks in  $\epsilon_2(\omega)$ . The shoulder peak at around 4 eV may be attributed to the transitions : O  $2p$  at  $\rightarrow$  Ti  $3d - t_{2g}$  and O  $2p \rightarrow$  Ti  $3d - e_g$  both at the  $\Gamma$  point. The high peak at 5 eV due to O  $2p \rightarrow$  Ti  $3d - e_g$  at the  $\Gamma$  point. A third shoulder peak at 6 eV is due to the transition O  $2p \rightarrow$  Ti  $3d - e_g$  also at the  $\Gamma$  point. As in the case of  $CaTiO_3$ , the structure in the high frequency part has both lower heights and are shifted to higher frequencies. The cause is the same as discussed above.

*BaTiO<sub>3</sub>* :

Lastly, let us look at figures 6-8. If we compare the shape of the imaginary part of the dielectric function  $\epsilon_2(\omega)$  obtained by our accurate estimate of the transition rate with that of [41], we note that agreement with experiment [42] is much better when we take the energy-frequency dependences of the transition matrix into account. The relative weights of the low frequency peaks, at 3.8 eV and 5 eV are correctly reproduced here.

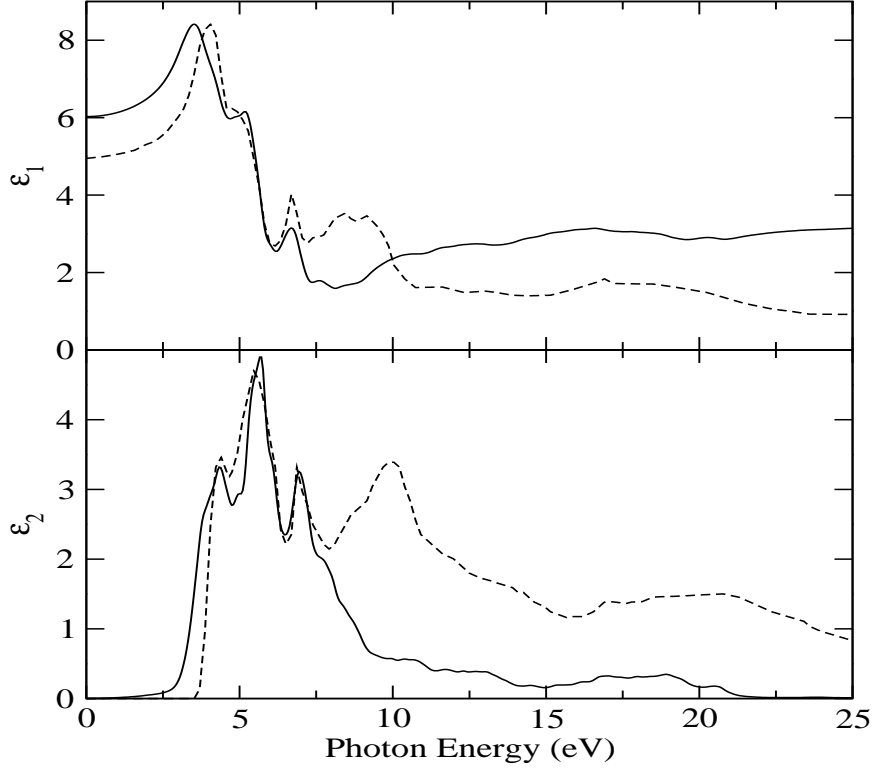


**Figure 6.** Comparison of calculated and experimental real part  $\epsilon_1(\omega)$ (top) and imaginary part  $\epsilon_2(\omega)$  (bottom) of dielectric function of  $CaTiO_3$  as a function of Photon energy: dotted line is experimental ([25]-[26]), continuous line is theoretical.

The lower peak is attributed to the transition from the O  $2p$  to the Ti  $3d-t_{2g}$  band and from the O  $2p$  to the Ti  $3d-e_g$  band both at the  $\Gamma$  points. The next higher peak is because of the transition from the O  $2p$  to the Ti  $3d-e_g$  band at the  $\Gamma$  point. Our present study also indicates a peak around 10 eV and the features at higher frequencies follow the experimental results closely, although the amplitude seems to have been underestimated as compared to the low frequency results. In all cases, although the lower frequency part is much better reproduced, the high frequency structures in the theoretical result is shifted upwards. As before, we argue that this is probably an artifact of the rigid shift of the scissors type approach. A energy-frequency dependent self-energy of the type given by the GW method should provide the necessary correction. In addition, the wrong heights at higher frequencies could also arise from the fact that we have neglected transitions to some of the higher energy conduction bands. A more complete, perhaps a three panel calculation at higher energies, should correct this. Alternatively, we could use the higher order NMTOs [43], when they are available, since they span a much larger energy range.



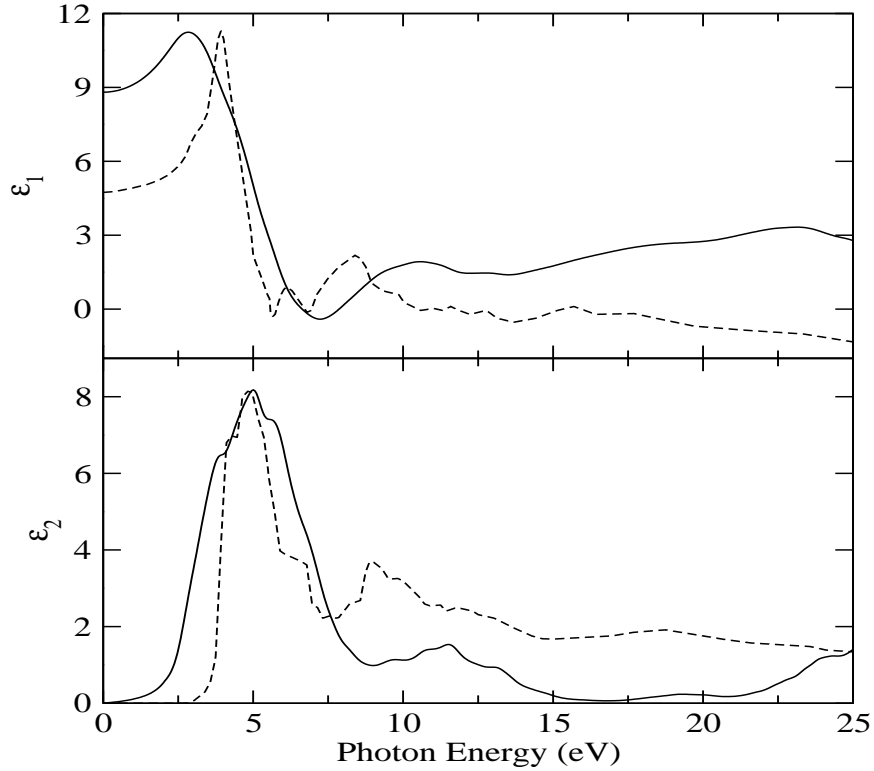


**Figure 7.** Comparison of calculated and experimental real part  $\epsilon_1(\omega)$ (top) and imaginary part  $\epsilon_2(\omega)$  (bottom) of dielectric function of  $SrTiO_3$  as a function of Photon energy: dotted line is experimental ([42]), continuous line is theoretical.

#### 4. Conclusion

We have proposed here a modified expression for the optical conductivity as a convolution of an energy-frequency dependent transition matrix and the energy resolved joint density of states. The main motivation was to generalize it to disordered systems, where the traditional reciprocal space formulation breaks down due to the failure of Bloch's Theorem. In order to be confident in our new formulation we have applied it here to the three alkaline earth perovskite titanates in their paraelectric phases. The results are in reasonable agreement with experimental data. The agreement is as good as we can expect from a LDA calculation. This formulation will now form the starting point of a two-fold generalization : first, combining with the ASR to random systems and as then as a starting point for a many-body GW formulation.

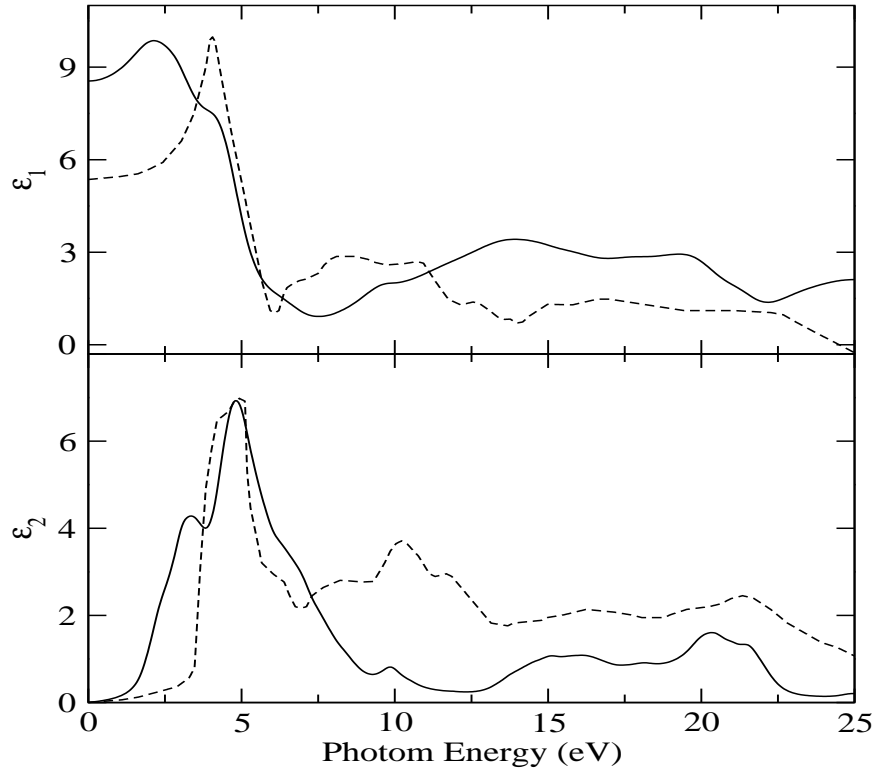


**Figure 8.** Comparison of Calculated and experimental real part  $\epsilon_1(\omega)$ (top) and imaginary part  $\epsilon_2(\omega)$  (bottom) of dielectric function of  $BaTiO_3$  as a function of Photon energy: dotted line is experimental ([42]), continuous line is theoretical.

## References

- [1] Mookerjee A., 1973 *J. Phys. C: Solid State Phys.* **6** 1340
- [2] Kaplan T. and Gray L.J., 1977 *Phys. Rev.* **B 15** 3260
- [3] Saha T., Dasgupta I. and Mookerjee A., 1996 *J. Phys.: Condens. Matter* **8** 1979
- [4] Dasgupta I., Saha T. and Mookerjee A., 1997 *J. Phys.: Condens. Matter* **9** 3529
- [5] Ghosh S., Das N. and Mookerjee A., 1999 *Int. J. Mod. Phys. B* **21** 723
- [6] Castet-Mejean L., 1986 *J. Phys. C: Solid State Phys.* **19** 1637
- [7] Michel-Calendini M. and Mesnard G., 1971 *Phys. Stat. Sol.* **44** K117
- [8] Michel-Calendini M. and Mesnard G., 1973 *J. Phys. C: Solid State Phys.* **6** 1709
- [9] Kahn A.H. and Leyendeker A.J., 1964 *Phys. Rev.* **135** A1321
- [10] Mattheiss L.F., 1972 *Phys. Rev.* **B6** 4718
- [11] Soules T.F., Kelly E.J., Vaught D.M. and Richardson J.W., 1972 *Phys. Rev.* **B6** 1519
- [12] Battaye F.L., Hochst H. and Goldmann A., 1976 *Solid State Commun.* **19** 269
- [13] Pertosa P. and Michel-Calendini F.M., 1978 *Phys. Rev.* **17** 2011
- [14] Perkins P.G. and Winter D.M., 1983 *J. Phys. C: Solid State Phys.* **16** 3481
- [15] Zook D.J. and Casselman T.M., 1975 *Surf Sci* **27** 244
- [16] Soules T.F., Kelly E.J., Vaught D.M. and Richardson J.W., 1972 *Phys. Rev.* **B6** 1519
- [17] Cohen R.E., Krakauer H., 1990 *Phys. Rev.* **B42** 6416 ; 1992 *Ferroelectrics* **136** 65
- [18] Cohen R.E., 1992 *Nature* **358** 136
- [19] Singh D.J. and Boyer L.L., 1992 *Ferroelectrics* **136** 95
- [20] King-Smith R.D. and Vanderbilt D., 1994 *Phys. Rev.* **B49** 5828 ; 1992 *Ferroelectrics* **136** 85
- [21] Andersen O. K. 1975 *Phys. Rev. B* **12** 3060

- [22] Jepsen O. and Andersen O. K. 1971 *Solid State Commun.* **9** 1763
- [23] Skriver H. L. 1984 *The LMTO Method: Muffin Tin Orbitals and Electronic Structure* (New York: Springer)
- [24] Saha K.K., Saha-Dasgupta T and Mookerjee A, 2001 (to be submitted in *J. Phys.: Condens. Matter* )
- [25] Ueda K., Yanagi H., Hosono H. and Kawazoe H. 1998 *J. Phys.: Condens. Matter* **10**, 3669
- [26] Ueda K., Yanagi H., Hosono H. and Kawazoe H. 1999 *J. Phys.: Condens. Matter* **11**, 3535
- [27] Uspenski Yu A., Maksimov E.G., Rashkeev S.N. and Mazin I.I., 1983 *Z. Phys.* **B 53** 263
- [28] Alouani M., Koch J.M. and Khan M.A., 1986 *J. Phys. F: Met. Phys.* **16** 473
- [29] Alouani M., Brey L. and Christensen N.E., 1988 *Phys. Rev.* **B 37** 1167
- [30] Zemach R., Ashkenazi J. and Ehrenfreund E., 1989 *Phys. Rev.* **B 39** 1884
- [31] Zemach R., Ashkenazi J. and Ehrenfreund E., 1989 *Phys. Rev.* **B 39** 1891
- [32] Hobbs D., Piparo E., Girlanda R. and Monaca M., 1995 *J. Phys.: Condens. Matter* **7** 2541
- [33] Mo S.D., Ching W.Y., Chisholm M.F. and Duscher G., 1999 *Phys. Rev.* **B 60** 2416
- [34] Kimura S., Yamaguchi Y., Tsukada M. and Watanabe S., 1995 *Phys. Rev.* **B 51** 11049
- [35] Wemple S.H., 1970 *Phys. Rev.* **B 2** 2679
- [36] Cardona M., 1965 *Phys. Rev.* **146** A651
- [37] Harrison W.A., *Electronic Structure and the Properties of Solids* (Dover, New York, 1989) Chapter 19
- [38] Wolfram T. and Ellialtıođlu Ő., 1977 *Phys. Rev.* **B 15** 5909 ; 1982 *Phys. Rev.* **B 25** 2697
- [39] Saha S., Sinha T. P. and Mookerjee A. 2000 *Phys. Rev.* **B 62**, 8828
- [40] Saha S., Sinha T. P. and Mookerjee A. 2000 *J. Phys.: Condens. Matter* **12**, 3325
- [41] Saha S., Sinha T. P. and Mookerjee A. 2000 *Eur. Phys. J. B* **18**, 207
- [42] Bäuerle D., Braun W., Saile V., Sprussel G. and Koch E. E. 1978 *Z. Phys.* **B 29** 179
- [43] Andersen O.K. and Saha-Dasgupta T. 2000 *Phys. Rev.* **B 62**, R16219